Full-wave Optimization of Large Compact Antenna Test Ranges

Oscar Borries, Erik Jørgensen, Peter Meincke, Hans-Henrik Viskum
TICRA, Copenhagen, Denmark
{ob,ej,pme,hhv}@ticra.com

***Abstract*—The challenges related to the increasing physical size of satellite platforms carry over to a number of related areas, including the design of Compact Antenna Test Ranges (CATRs) capable of handling such structures. In the present paper, we consider the design of a large CATR and use state-of-the-art Computational Electromagnetics (CEM) software, based on full-wave methods to fully include the important diffraction effects, to perform various parameter studies and ultimately allow full-scale optimization of a CATR.**

I. Introduction

In recent years, the increased payload capabilities of modern launchers have allowed satellites of unprecedented size. This increased satellite size allows for much better performance of the subsystems on the satellite, but proves to be quite a challenge for some of the other processes in satellite design, including manufacturing and testing.

This is particularly true when measuring the far-field behaviour of the antennas. While initial measurements may be carried out using smaller ranges, later testing phases require the full effects of the satellite platform and thus must be performed in ranges with sufficently large quiet zones (QZs).

The design of ranges with such large QZs is a challenge. Aside from significant manufacturing constraints, designing such as system to provide strong QZ performance throughout the frequency range is difficult. For high frequencies, the extreme electrical size requires very long computation times even when using asymptotic methods, while at lower frequencies, the often complicated geometry means that full-wave solvers have to be applied, resulting in high memory consumption.

In the present paper, we demonstrate how some of the recent developments in CEM tools, implemented in the latest version of TICRAs flagship product GRASP, allows significant performance benefits to be obtained when designing a CATR. The paper begins with a brief discussion of the analysis methods involved, and how they are accelerated, and then moves on to a description of the initial design of a CATR. We then continue to improve the design by subjecting various parameters to an optimization, and present our conclusions.

II. Analysis Methods

There are three main approaches for analysing CATRs, depending on the required accuracy and electrical size of the system.

A. Geometrical Optics

Geometrical Optics (GO), possibly including diffraction by means of Uniform Theory of Diffraction (UTD), has previously been a common analysis tool for CATR, particularly when applying optimization [1]. With the progress in computing resources and CEM algorithms, it appears to be used less frequently, at least for the later stages of the design process. However, it still has several key features that justify its use in CATR design:

- Strictly speaking, its time and memory requirements are independent of the frequency. As such, for extreme electrical sizes, it can be the only option.
- By disregarding UTD and only tracing reflected rays, GO can allow users to gauge the "ideal" performance of the system, i.e. if no diffraction is present. This approach has been used in the literature [2], and can allow more efficient optimization by subtracting the feeds amplitude taper from the quiet zone performance, isolating the amplitude ripples due to diffraction.

B. Physical Optics/Physical Theory of Diffraction

A popular algorithm for the analysis of CATRs [3], and reflectors in general, is Physical Optics (PO), combined with Physical Theory of Diffraction (PTD). While still an asymptotic method, like GO/UTD, it is very accurate for large, smooth structures. Unfortunately, it is typically much more time-consuming than GO/UTD.

For Physical Optics on electrically large structures, GRASP is recognized as an industry leading tool, due to its use of customized sparse integration rules, which reduce the number of samples of the integrand. This results in much faster computation. However, the main caveat of PO remains: The computational time generally scales as $\mathcal{O}(f^4)$, where f is the frequency, such that doubling the frequency means that the computation takes 16 times longer. To reduce this scaling, there has been a large effort in recent years to develop accelerated algorithms, also called "fast" algorithms, that reduce the scaling of PO to $\mathcal{O}(f^2 \log f)$, similar to how the FFT reduces the scaling of the discrete Fourier transform. While some "Fast-PO" algorithms were published in the last decade, it was only recently [4] that algorithms were presented that provided both sufficient speed-up and accuracy to allow their use in the design of high-accuracy systems such as a modern CATR. These algorithms have been implemented in GRASP 10.5.

TABLE I
PARAMETERS FOR THE CATR SETUP WITH INITIAL VALUES.

Feature	Symbol	Starting Value
Total footprint	D	$2S + L = 7.5\,\mathrm{m}$
Serration Length	S	$1\,\mathrm{m}$
Main reflector edge length	L	$5.5\,\mathrm{m}$
Number of serrations	N	10
Serration Width	L/N	$0.55\,\mathrm{m}$
Frequency	f	$1.5\,\mathrm{GHz}$
Feed taper	F_t	-1 dB
Quiet zone diameter	Q	$4\,\mathrm{m}$
Quiet zone distance from vertex	Q_d	$12\,\mathrm{m}$
Focal length	F	$10\,\mathrm{m}$

C. Method of Moments

Method of Moments (MoM) is a full-wave method, meaning that it takes into account all physical phenomena. It works by discretizing the surface of the object using geometrical patches, and then represents the current on those patches using polynomial vector basis functions. MoM is accurate; the expected dynamic range of the implementation in GRASP is about 60 dB for the default accuracy, and the accuracy can be further improved if requested by the user. Since it takes into account all phenomena, but requires $\mathcal{O}(f^4)$ scaling of memory and computational time, it is typically used only on small-scale or simplified CATR models.

MoM can be accelerated by the Multi-Level Fast Multipole Method (MLFMM), which has $\mathcal{O}(f^2 \log f)$ scaling. MLFMM was implemented recently in GRASP, and was adapted to the efficient Higher-Order (HO) basis functions used in GRASP, which allow much lower memory requirements [5], [6] than implementations based on the widely used Rao-Wilton-Glisson (RWG) basis functions.

III. DESIGN

The initial design is a single-reflector CATR with a $4\,\mathrm{m}$ circular cylindrical quiet-zone. The footprint of the reflector is fixed at 7.5-by-7.5 meter as the fundamental constraint of the design. The frequency under consideration is $1.5\,\mathrm{GHz}$. While we note that a compensated dual-reflector system is often preferred for full spacecraft testing, due to stronger performance characteristics, space considerations may not allow for the design of such a large system and we therefore focus on single-reflector systems. Further, recent scientific progress [7] has allowed for much better performance of single reflector CATR than was previously possible.

The basic design is illustrated in Fig. 1 and the key parameters are shown in Table I.

A. Quality of QZ

Determining a quality estimate of a CATR design, needed for optimization, is not straight-forward and indeed does not have a unique answer. In the literature, it is most common to find quality estimates based on the quiet-zone field. For instance, one can perform a GO analysis (without diffraction, i.e. a simple projection of the feed image into the quiet zone) to find the taper of the feed in the QZ. Then, one can compute

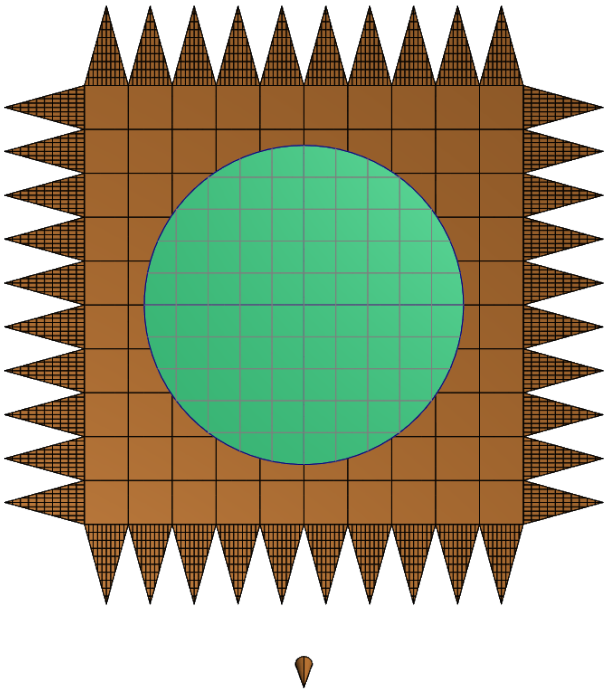

Fig. 1. Starting configuration. Circular plate in quiet zone shown in green.

(by either PO/PTD or MoM/MLFMM) the scattered field $\boldsymbol{E}$ from the CATR system in the QZ. The key performance metric κ is then:

$$\boldsymbol{F} = \boldsymbol{E} - \boldsymbol{G}, \tag{1}$$

$$\kappa = \max(10\log_{10}(|\boldsymbol{F}|)) - \min(10\log_{10}(|\boldsymbol{F}|)), \tag{2}$$

where $\boldsymbol{G}$ is the GO field in the QZ. Thus, κ is the peak-to-peak amplitude ripple in dB in the quiet-zone, after the feed taper has been subtracted.

However, this approach completely disregards the amplitude taper in the quiet-zone by subtracting it from the quality estimate κ, since the peak-to-peak ripple would otherwise be lost to the more significant amplitude taper. Furthermore, the peak-to-peak ripple κ can be hard to translate into the quality of the measured pattern one would achieve.

Instead, we apply the following approach, inspired by [8]. First, we place a circular plate of diameter $4\,\mathrm{m}$ in the quiet-zone, and compute an overdiscretized "true" far-field from this antenna as illuminated by a plane-wave. Then we compute the coupling between the CATR and the antenna as we rotate the antenna — by reciprocity, this yields the far-field pattern that would be measured if that specific antenna were measured using that specific CATR. We call this far-field pattern the computed measured field. We can then compare these two patterns by computing the Relative RMS Error, defined as

$$\text{Relative RMS Error} = \sqrt{\frac{\sum_{i=1}^{N_s} |\boldsymbol{E}_{i,\text{true}}|^2 - |\boldsymbol{E}_{i,\text{calc}}|^2}{\sum_{i=1}^{N_s} |\boldsymbol{E}_{i,\text{true}}|^2}}, \tag{3}$$

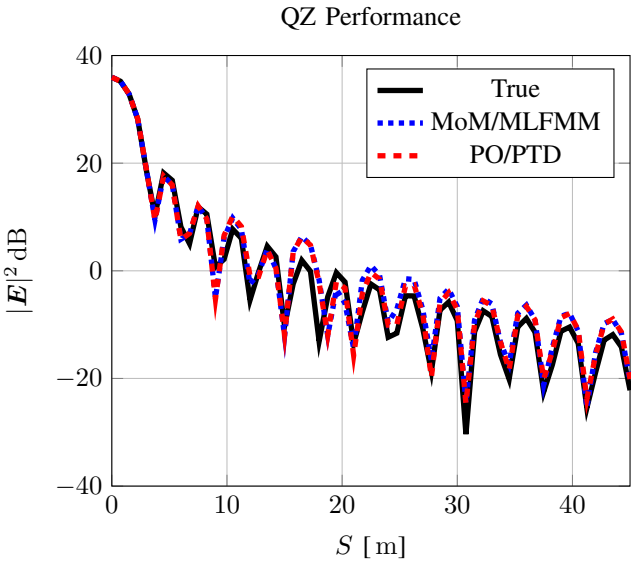

Fig. 2. True far-field (in red) from a circular plate placed in the quiet-zone vs. the simulated measured far-field from both PO and MoM/MLFMM.

where $\boldsymbol{E}_{i,\text{true}}$ and $\boldsymbol{E}_{i,\text{calc}}$ denote the electric far field at the i^{th} sample point from the true and computed measured fields respectively, and N_s is the number of samples.

In the measurement literature, this number is often expressed as the equivalent noise level:

$$\varrho = 20\log_{10}\left(\text{Relative RMS Error}\right) \tag{4}$$

For 1.5 GHz, both PO/PTD and MoM/MLFMM are applicable. As a starting point for the design process, we compute κ using both methods:

$$\kappa_{PO/PTD} = 0.68\,\text{dB}, \tag{5}$$

$$\kappa_{MoM} = 0.71\,\text{dB}. \tag{6}$$

Again, while these numbers are useful in quantifying part of the performance of a CATR, it is not suitable for use as an optimization goal.

Further, we consider the Equivalent noise level achieved to allow a comparison between the two quality estimates:

$$\varrho_{PO/PTD} = -56.63\,\text{dB}, \tag{7}$$

$$\varrho_{MoM} = -57.19\,\text{dB}. \tag{8}$$

The simulated measured cuts on which these ϱ numbers are based are shown in Fig. 2. We see a fairly good agreement between PO/PTD and MoM/MLFMM, although some of the secondary sidelobes vary somewhat. The large deviation that both MoM/MLFMM and PO/PTD has from the true far-field pattern at around $\theta = 17°$ is caused by the focus of the circular plate pointing directly at the serrations, and thus getting the maximum contribution from the diffractions.

IV. Optimization

The optimization of CATR is a challenging problem, mainly because of the long computation times (at least for full-wave analysis) and the potential for local minima. This suggests the use of specially tailored optimization algorithms that take great care in reducing the number of function evaluations while searching for global minima, typically known as "Efficient Global Optimization" algorithms [9]. A number of these algorithms exist, and we provide an outline of our implementation below:

1) Start: Choose a low number of points, called 'sites', in which to evaluate the RMS function.
2) Based on those sites, build a surrogate model using e.g. Kriging [10], evaluate the model accuracy.
3) **while** (not accurate enough)
   a) Find a region where the surrogate model should be more accurate.
   b) Add a site in that region to the surrogate model.
   c) Reevaluate the accuracy of the model.
4) **end while**
5) Optimize the surrogate model using a global optimization algorithm.

It is important to note that each of the points listed above require careful consideration — everything from the choice of the surrogate model, the evaluation of model accuracy, the method of finding the best site to add to a model, and indeed the choice of global optimization algorithm at the end, can be adapted to suit the specific task at hand. For more details, we refer to [11].

V. Results

A. Serration length

With the starting point for the optimization described above, we begin by performing a brief study of the length of the serrations S. In Fig. 3, we vary the serration length between 0.4 m and 1.8 m, corresponding to $2\lambda - 9\lambda$, in 16 discrete steps. Further, we compute a Kriging surrogate model using the DACE toolbox [12] based on 9 of the sites. As the figure shows, the resulting surrogate model fits very well with the true results. Moreover, the results indicate that the best performance is achieved by having serrations of roughly 4λ-6λ length, consistent with practical experience. Finally, the figure shows that while PO can provide a reasonable approximation for some cases, it is too inaccurate for the final stages of optimization, with the minimum overestimating the optimal serration length by about 1λ.

B. Feed taper

We now consider both the feed taper F_t at the edge of the serrations as well as the serration length S simultaneously. By computing a grid of 16 x 16 points, and using a 9 x 9 grid of sites to construct a surrogate model, we can evaluate the accuracy of the Efficient Global Optimization approach on a 2D problem, yielding a surrogate model with a Relative RMS compared to the true grid of 3%.

The grid is seen in Fig. 4. We further apply a DACE model to this, and then use Efficient Global Optimization to find the minimum at $S = 1.248$, $F_t = -1.67$ dB yielding a Equivalent

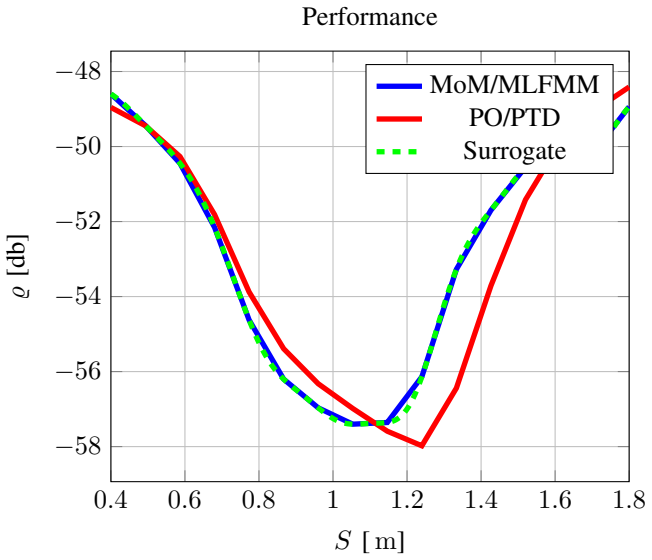

Fig. 3. Performance as function of serration length S.

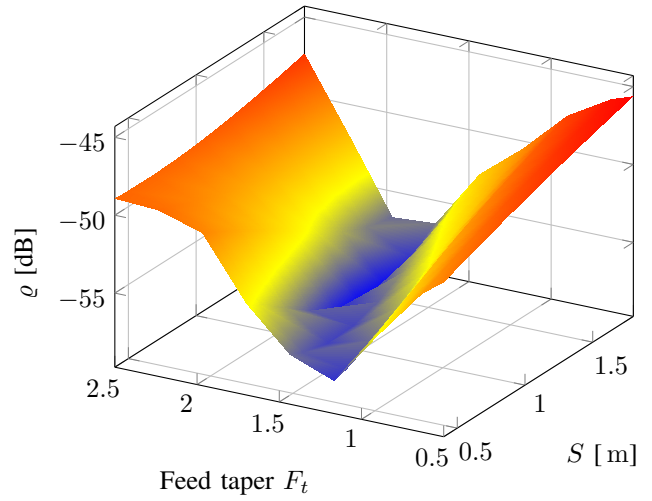

Fig. 4. Performance as function of both serration length S and feed taper F_t.

noise level of $\varrho = -58.48\,\mathrm{dB}$. The corresponding design is shown in Fig. 5, and the resulting pattern is shown along with the true pattern in Fig. 6.

C. Advanced optimization

We now consider a more complete scenario, fixing the feed taper at $F_t = -1.67\,\mathrm{dB}$ and focusing on the serration shape. To improve the serration performance, we introduce a model of the serrations with five variables, as shown in Fig. 7. We also introduce a linear slant, such that the serrations at the center of the rim edge are isosceles triangles, while at the edges of the rim, they are right-angled. This should yield a better performance based on theoretical studies [13].

Based on applying the Efficient Global Optimization, we obtain the values $[y_1, y_2, y_3, y_4, y_5] = [0.099, 0.635, 0.720, 0.994, 1.255]$, yielding a Equivalent

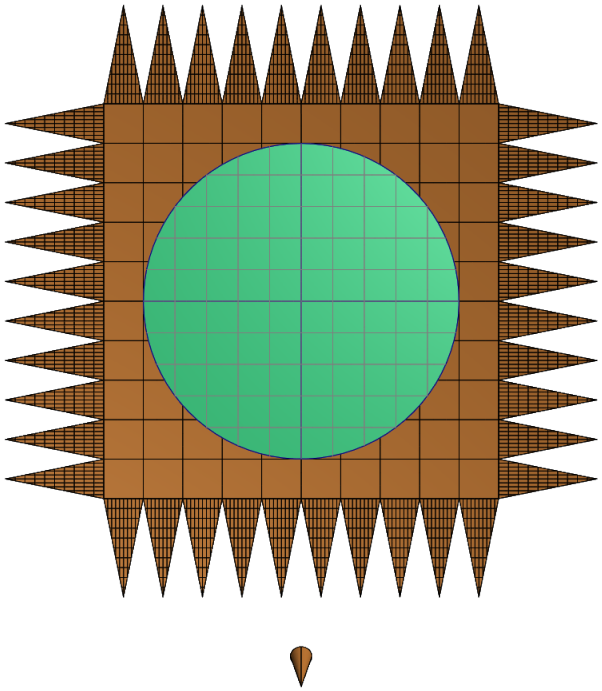

Fig. 5. Optimum configuration when optimizing for S and F_t. Circular plate in quiet zone shown in green.

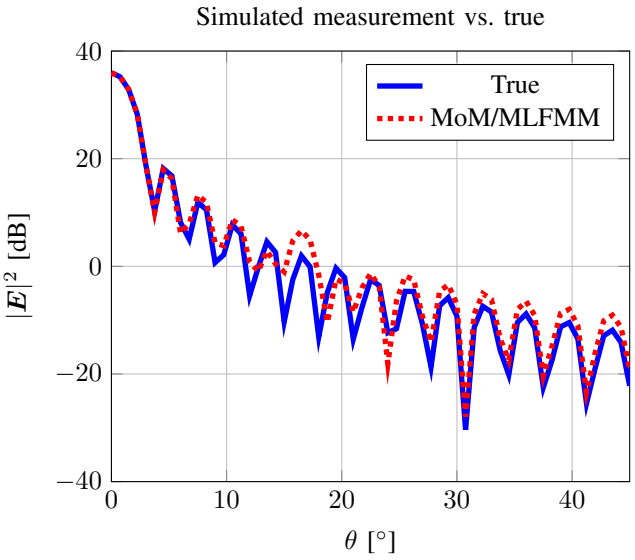

Fig. 6. True vs. computed measured fields for the optimized S and F_t. While the ϱ is only about 1 dB better than the initial design, comparison with Fig. 2 shows a noticeable improvement on the first few sidelobes.

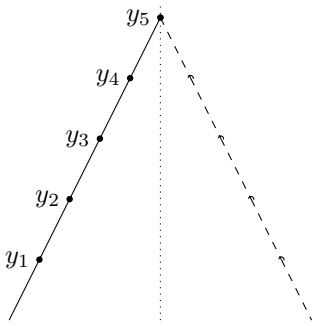

Fig. 7. Model of serrations using five variables, y_1, y_2, y_3, y_4, y_5, indicating the height of the nodes relative to the reflector rim. The left side line is then reflected across the center. While the points in this illustration lie on a straight line, the points are connected by a spline to allow a curved edge of the serrations.

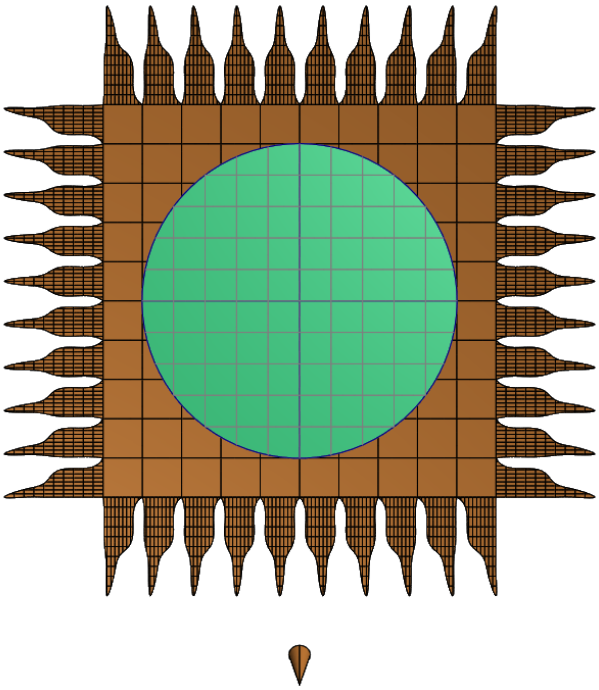

Fig. 8. Optimum configuration when optimizing for the spline shape. Circular reflector in quiet zone shown in green.

noise level of $\varrho = -63.82\,\mathrm{dB}$ from the design shown in Fig. 8 and the results shown in Fig. 9.

VI. Conclusion

We have shown how recent progress in CEM algorithms allow for full-wave analysis of real-size compact antenna test ranges with very brief simulation times. This further opens up the possibility for semi- or even fully automated optimization approaches, potentially allowing for better CATRs at low frequencies.

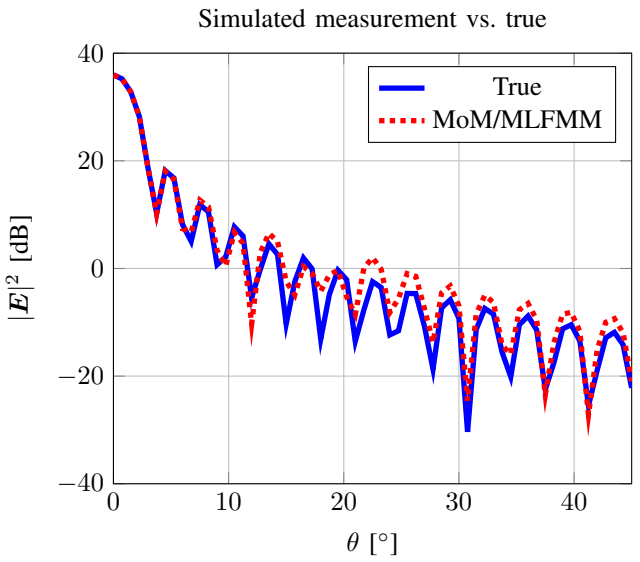

Fig. 9. True vs. computed measured fields for the optimized serrations. The ϱ is about 6.5 dB better than the initial design. Comparing with Fig. 2 shows a strong improvement.

References

[1] J. Hartmann and D. Fasold, "Improvement of Compact Ranges by Design of Optimized Serrations," in *Millenium Conference on Antennas and Propagation*, Davos, Switzerland, 2000, pp. 1–4.

[2] I. J. Gupta, K. P. Ericksen, and W. D. Burnside, "A Method to Design Blended Rolled Edges for Compact Range Reflectors," *IEEE Transactions on Antennas and Propagation*, vol. 38, no. 6, pp. 853–861, Jun. 1990.

[3] C. H. Schmidt, A. Geise, J. Migl, H.-J. Steiner, and H.-H. Viskum, "A Detailed PO/PTD GRASP Simulation Model for Compensated Compact Range Analysis with Arbitrarily Shaped Serrations," in *Antenna Measurement Techniques Association*, Oct. 2013, pp. 6–11.

[4] O. Borries, H. H. Viskum, P. Meincke, E. Jørgensen, P. C. Hansen, and C. H. Schmidt, "Analysis of Electrically Large Antennas using Fast Physical Optics," in *European Conference on Antennas and Propagation*, Lisbon, Portugal, Apr. 2015.

[5] E. Jørgensen, J. Volakis, P. Meincke, and O. Breinbjerg, "Higher Order Hierarchical Legendre Basis Functions for Electromagnetic Modeling," *IEEE Transactions on Antennas and Propagation*, vol. 52, no. 11, pp. 2985–2995, Nov. 2004.

[6] O. Borries, P. Meincke, E. Jørgensen, and P. C. Hansen, "Multilevel Fast Multipole Method for Higher-Order Discretizations," *IEEE Transactions on Antennas and Propagation*, vol. 62, no. 9, pp. 4695–4705, Sep. 2014.

[7] J. Pamp, R. Cornelius, D. Heberling, L. J. Foged, A. Giacomini, and A. Riccardi, "Reduction of the Cross Polarization Component in the Quiet Zone of a Single Reflector CATR," in *AMTA*, Oct. 2015, pp. 1–5.

[8] F. Jensen and K. Pontoppidan, "Modeling of the antenna-to-range coupling for a compact range," in *Proceedings of the Antenna Measurements Symposium*, 2001.

[9] D. R. Jones, M. Schonlau, and W. J. Welch, "Efficient Global Optimization of Expensive Black-Box Functions," *Journal of Global Optimization*, pp. 455–4492, 1998.

[10] D. Krige, "A statistical approach to some basic mine valuation problems on the Witwatersrand," *Jnl C'hem Met and Min Soc S Afr*, 1951.

[11] A. I. J. Forrester, A. Sobester, and A. J. Keane, *Engineering Design via Surrogate Modelling - A Practical Guide*. Wiley, 2008.

[12] H. B. Nielsen, S. N. Lophaven, and J. Søndergaard, "DACE - A Matlab Kriging Toolbox," Tech. Rep., 2002.

[13] F. Jensen, "Polarisation Dependent Scattering from the Serrations of Compact Ranges," in *Antenna Measurement Techniques Association*, Nov. 2007, pp. 150–155.